

A WIND-TUNNEL INVESTIGATION OF THE WIND SPEED AND TURBULENCE CHARACTERISTICS CLOSE TO THE GROUND OVER VARIOUS ESCARPMENT SHAPES

A. J. BOWEN and D. LINDLEY

Department of Mechanical Engineering, University of Canterbury, Christchurch, New Zealand

(Received 10 May, 1976)

Abstract. A wind-tunnel investigation of the wind flow over two-dimensional forward-facing escarpments is reported as part of a continuing research programme into the effects of local topography on the wind flow close to the ground. Four sharp-edged escarpments with their slopes varying between a cliff and a 4 : 1 gradient, were placed normal to a simulated neutrally-stable rural boundary layer which was modelled to a scale of 1 : 300. The resulting flows close to the surfaces of the escarpments were measured with a hot-wire anemometer. The modifications to the mean wind speed, turbulence intensity and energy spectra over the escarpments are described. The results indicate the extent and magnitude of the modification to the flow and suggest that significant changes in turbulence characteristics only occur in the wake region close behind the crest, where a shift of energy to higher frequencies is evident.

1. Introduction

An understanding of the modification to the earth's boundary layer caused by abrupt changes in local topography is essential if the local wind conditions at a site in hilly terrain are to be predicted. Wind speeds and turbulence data are well established for the neutral boundary layer over homogenous terrain (ESDU 1972, 1974), but very little quantitative information exists on the effect of hills on the local wind characteristics. Existing meteorological data are mostly confined to airports and populated areas situated on flat even terrain and any predictions of the wind flow over nearby hills are hazardous without extensive on-site measurements.

A major application of the understanding of topographical effects is in the estimation of wind loads on buildings and structures that are situated on exposed hill sites. In addition to the design of buildings in hilly urban areas, there are many other structures such as communication aerials, cable ways, and electricity transmission lines and towers, which are often sited on exposed ridges and whose structural reliability is of the utmost importance. Some building codes such as the British Standard CP3 (1972) and the New Zealand Standard 4203 (1976) apply to sites on uniform flat terrain and offer a simple wind speed exposure factor between 0.9 and 1.3 for hilly sites. In addition, special consideration has been given to sites near the crest of an escarpment by increasing the effective height of the building for the purpose of choosing a more appropriate design wind speed. A building close to the crest of a steeply sloping escarpment would thus have an effective height equal to the building height plus a fraction of the escarpment height, resulting in the choice of a higher design wind speed. Recent model and field tests by de Bray (1973), Freeston (1974) and Bowen and Lindley (1974) have confirmed the inadequacy of these factors to cope with the modification to the mean wind speed by escarpments and

showed that both the velocity increase and the extent of their influence downstream could be significantly greater than the ranges quoted in the above Codes. In addition, there is very little guidance given in the literature on the prediction of the turbulence characteristics that might prevail over a particular hill and that would enable maximum gust speeds and dynamic loading effects to be predicted for exposed sites.

A further application of topographical wind effects is in the optimum siting of wind turbines for the generation of power, where an increase in wind speed on a hill-top site compared with that on flat terrain could be used to advantage by enhancing the power output of a particular machine. A 50% increase in wind velocity results in over a 300% increase in available wind energy. Knowledge of the effects of hills on the wind flow would enable potential wind-turbine sites to be located and instrumented for more detailed wind surveys. In addition, a better prediction of the maximum loads on the turbine tower and blades under a variety of wind conditions would also be possible.

The modification to the mean wind speed at a particular height above local ground level over the hill can be expressed as the amplification factor A_z , defined as the mean wind speed at a height Z above local ground level divided by the mean wind speed of the undisturbed flow at the same height above the local flat ground, upstream of the hill. The amplification factor is then a direct measure of the increase in exposure of a structure due to its siting on the hill rather than on flat terrain.

It is recognised that every hill has a unique shape and situation that has made the development of generalised theories rather difficult and that field measurement for each case is the only reliable way of investigating a proposed site at the present time. Examples of field measurements in hilly terrain such as given in WMO No. 63 (1964) and Mitsuta (1971) are scarce and cover such a wide range of topographic situations and weather conditions that only the broadest generalisations can be concluded from them. Theoretical solutions such as Jackson (1975) give a good indication of the trends over two-dimensional obstructions but require field and model tests to confirm their quantitative results. In order to gain a better understanding of the topographical effects on wind flow, a project (Lindley *et al.*, 1974) was undertaken to develop field equipment that would enable full-scale measurements of wind-speed profiles and turbulence characteristics to be made over various hills and topographic situations. It was decided to concentrate initially on two-dimensional forward-facing escarpments in strong neutrally-stable winds, but at a later stage it is planned to use the field equipment to investigate more complex three-dimensional topography. Because of the inherent difficulties associated with field measurements, the wind-tunnel model tests reported here were carried out on various escarpment shapes to locate the best measuring positions and to provide model test results with which the field recordings could be compared.

2. Test Procedure

The tests were carried out in the 1.3 m \times 1.3 m boundary-layer wind tunnel at the University of Canterbury, a facility which has been described by Raine (1974). The

floor of the 12-m long working section was lined with a uniform roughness element of 3-mm height with four additional trip fences to reinforce the large-scale turbulence in the upper part of the boundary layer. The two-dimensional forward-facing escarpments were placed normal to the flow and spanned the full width of the tunnel. The model height of $H = 50$ mm represented 5% of the boundary layer and gave a tunnel blockage close to 4%. However, a zero longitudinal pressure gradient was maintained over the models by adjusting the height of the wind-tunnel roof; consequently, the effects of blockage on the measured velocities were considered to be small. The forward faces of the escarpments represented a cliff with slope angles of $\tan^{-1} 1$, $\frac{1}{2}$ and $\frac{1}{4}$. In order to preserve as far as possible the uniformity in surface roughness, all ground surfaces except for the cliff face were covered by the 3-mm roughness elements.

Measurements of the flow were made with a linearised hot-wire anemometer employing a single horizontal probe sensitive to the longitudinal and vertical velocity components of the flow. It was considered that the readings obtained by this probe configuration, which represented the total down-wind velocity component, adequately indicated the relevant flow velocity over the escarpments for engineering applications. The total down-wind velocity component that was recorded is represented throughout this paper by the mean flow velocity \bar{V}_z and the RMS of the fluctuating velocity by the subscript u . The mean flow would have had a significant vertical component close to the escarpment slopes, but elsewhere it could be considered as horizontal. Flow measurements were taken over the model escarpment at successive sites between $10 H$ upstream and $10 H$ downstream of the slope for each of the four models considered. A third-octave spectral-analyzer with a range between 2 and 10 000 Hz was used for the turbulence energy analysis.

3. The Undisturbed Boundary Layer

The undisturbed boundary layer upstream of the models was 1 m deep ($\delta = 1000$ mm) and was similar to that found in the field over open country, with a power-law exponent close to $\frac{1}{6}$ and a model scale of 1:300. The turbulence characteristics of the flow agreed with those previously recorded by Raine (1974). The turbulence intensity σ_u/\bar{V}_z slowly decreased with height from 0.25 at $Z = 10$ mm to 0.16 at $Z = 100$ mm, which also fitted the design data given by ESDU 72026 (1972) for a rural boundary layer modelled to a scale of 1:300. Sample measurements using a cross-wire probe gave satisfactory ratios of horizontal and vertical components of turbulence intensity to the friction velocity of 2.50:1 and 1.25:1, respectively, close to the ground. The non-dimensional turbulent energy spectral density for the along-wind component $n \cdot S_{uu}(n)/\sigma_u^2$, is shown in Figure 1 for one escarpment height above local ground level. The von Kármán spectrum for the horizontal velocity component of a rural boundary layer at the same height (surface roughness parameter $Z_0 = 0.1$ m; $^*L_u = 75$ m) is included for comparison and satisfactory agreement is achieved if a model scale of 1:300 is again assumed. The integral length scales of turbulence *L_u , that were derived from the peak

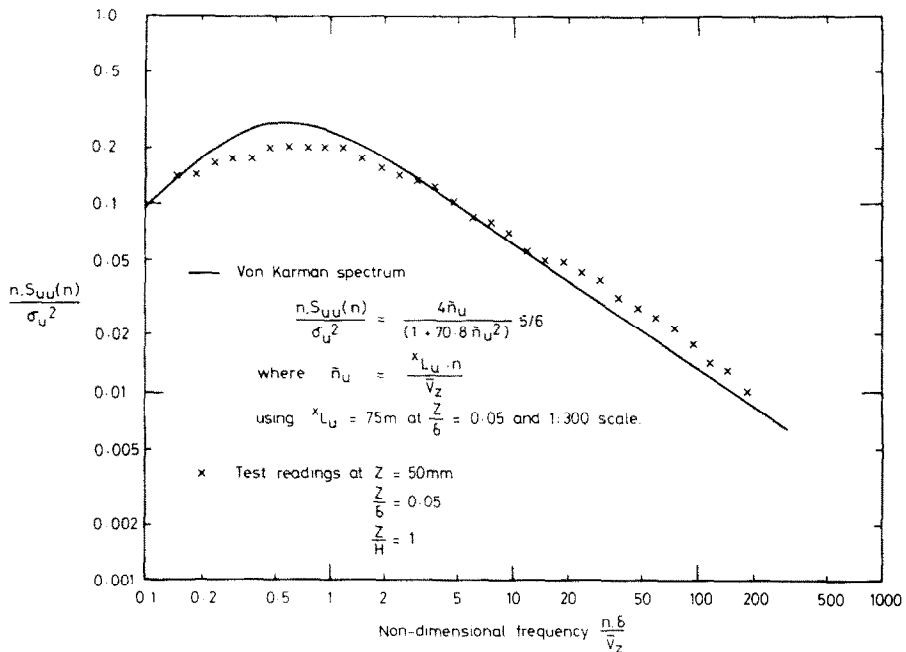


Fig. 1. The turbulent energy spectral density of the undisturbed upstream flow at a height equal to the escarpment height, compared with the standard von Kármán spectrum.

spectral frequency, were similar to those found by integration of the autocorrelation-delay time curves. Typical values were $xL_u = 120$ mm at $Z = 10$ mm and $xL_u = 400$ mm at $Z = 100$ mm, which showed the characteristic increase with height and also confirmed the choice of the 1:300 model scale.

4. The Flow over the Escarpments

Typical mean velocity-height profiles over the escarpments are shown in Figure 2 and are drawn for each location as a single trace for all four models because of the apparent insensitivity of the flow velocities to slope angle in the range of models considered. From these readings, the amplification factor A_z was calculated and first displayed in Figure 3 as height profiles for each position. The two extreme cases of slope considered are shown to indicate the range of values encountered. These profiles then established the contours of equal amplification factor which are shown in Figure 4 for the four escarpment models. The RMS velocity fluctuations that were measured over the models are shown in Figure 6 as σ_u/\bar{V}_∞ , for the two extreme cases of slope where \bar{V}_∞ is the free-stream flow velocity of 20 m s^{-1} . Little change in σ_u/\bar{V}_∞ is evident above $Z/H = 1$, but when expressed in Figure 7 as contours of equal turbulence intensity σ_u/\bar{V}_z , the variations become more substantial.

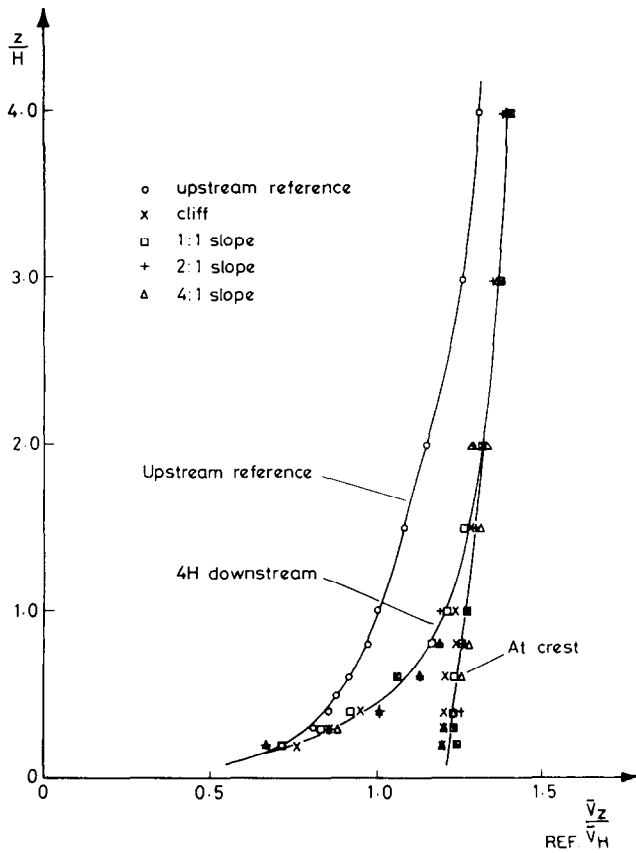
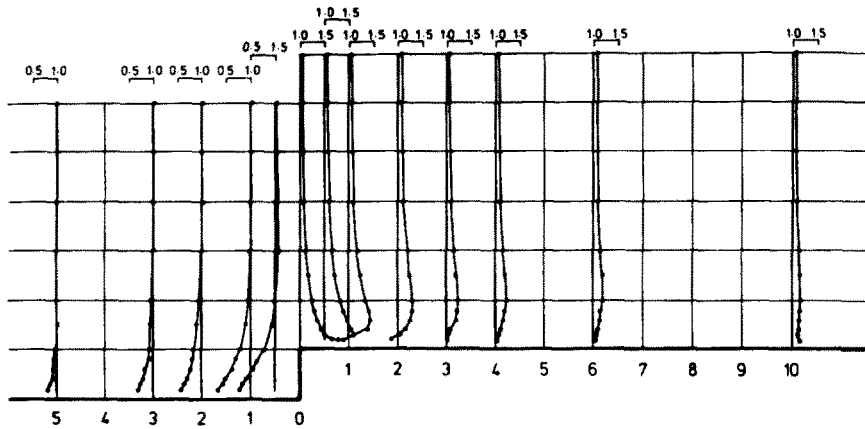


Fig. 2. Examples of normalised mean velocity-height profiles.

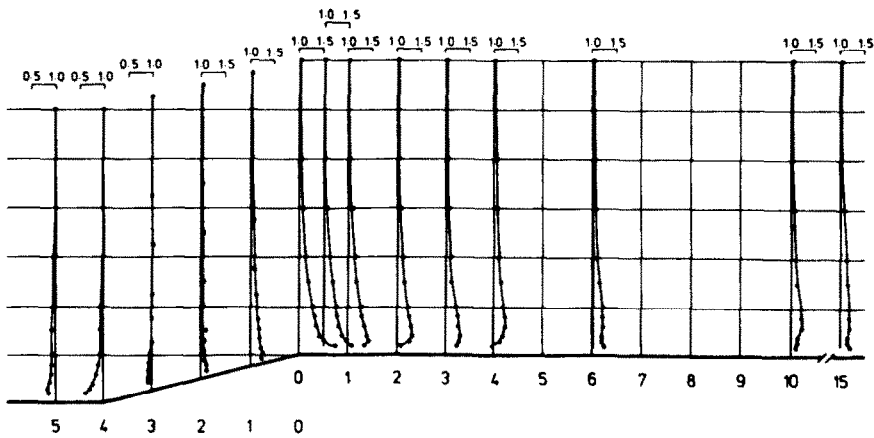
5. Discussion

5.1. MEAN FLOW

The flows over the four escarpments were similar in structure downstream of each crest, with the main difference occurring in the extent and intensity of turbulence in the wake close to the ground, immediately behind the crest. The small influence of the escarpment slope angle within the range of slopes investigated is evident particularly in the velocity-height profiles in Figure 2. Sacre (1973) observed that the major effect on the amplification factor A_z came from slope angles of less than 30° with predominantly unseparated flows, and steeper slopes had a decreasing influence on A_z which tended to a maximum value of between 1.4 and 1.5. For the near vertical slopes, the expected upstream vortex would provide an effective gradual slope for the main flow outside the separation streamline and consequently would reduce the influence of slope angle in this range.



(A) CLIFF



(B) 4:1 SLOPE

Fig. 3. (A), (B) Variation of the amplification factor with height over the cliff and a 4:1 sloping escarpment.

A certain degree of shelter is apparent (Figures 3 and 4), up to $5H$ upstream of the slopes where A_z was less than one, although the strength of the upstream vortex in front of the cliff face was not known. About one-third of the way up the slope in the rapidly accelerating flow, A_z reached unity and rapidly increased in value towards the crest. The velocity-height profiles at the crest were nearly uniform, which caused the value of A_z to increase rapidly towards the ground. An overall maximum value of A_z for the flow of between 1.7 and 1.8 was found for all four slopes at the lowest height ($Z/H = 0.2$) above the crest that was investigated. Other model escarpment tests by de Bray (1973), Sacre (1973) and Freeston (1974), showed similar trends in the mean flow variation with height at the crest, but peak values of A_z estimated from their results tended to be lower, often between 1.4 and 1.5. This discrepancy in the

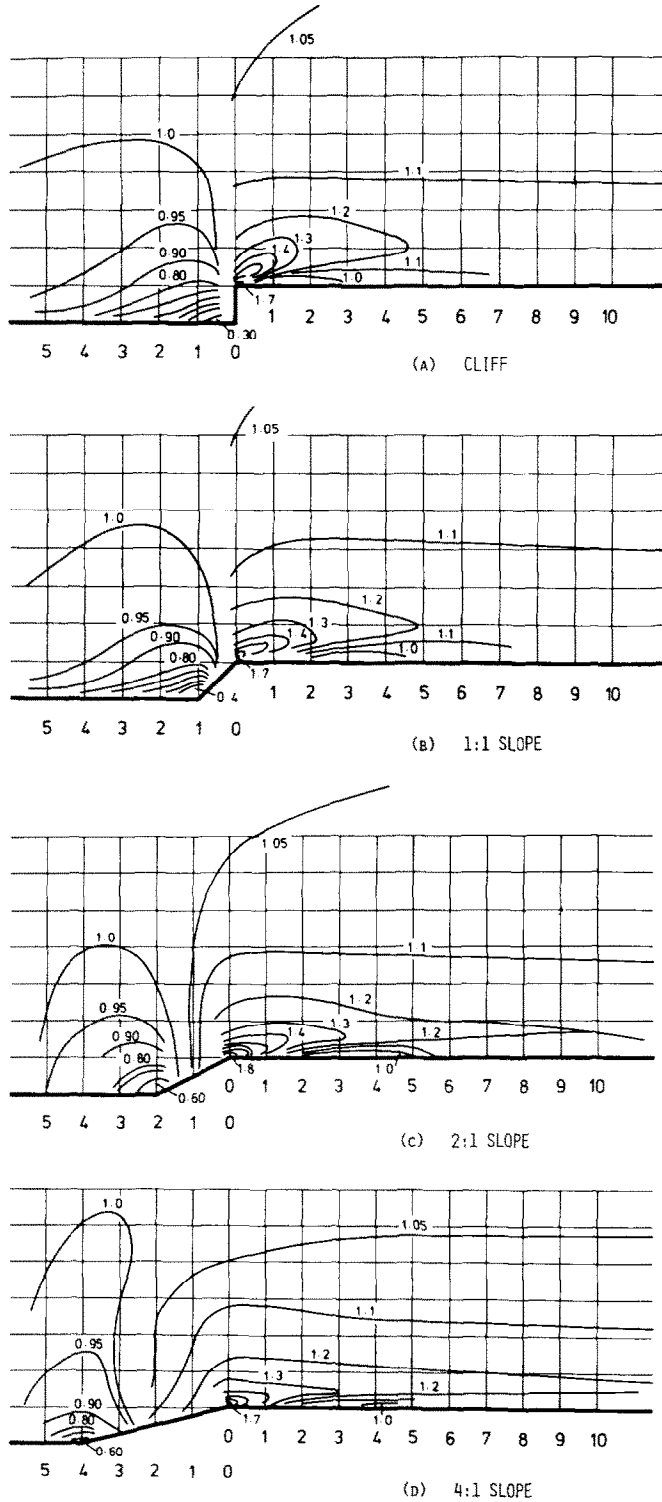


Fig. 4. (A)-(D) Contours of equal amplification factor over various escarpment slopes.

peak value of A_z is highlighted by the very rapid change in A_z with height close to the ground, where the measurement locations are close to the 3 mm high ground roughness elements used in the tests. In contrast, de Bray (1973) and Freeston (1974) used smooth escarpment models. The effective height above the displacement depth due to these roughness elements would have been 2 to 3 mm less than that indicated by the true height above ground, which at the lowest position was 10 mm. This reduction in effective height would have yielded higher values of A_z over an escarpment with a rough surface than that measured over a smooth model at the same height above ground level. Sacre (1973) used carpet of an unspecified depth to cover his models.

The major region of influence from the escarpments defined by $A_z > 1.1$ was confined to below a height of $3H$ above the local ground level. This region persisted beyond $10H$ downstream of the crest for all four slopes considered, as noted previously in field tests described by Bowen and Lindley (1974). Downstream of the crest, a wake region of high shear and lower mean velocities grew from the crest and extended to a height of about $1H$ for the cliff and $0.4H$ for the 4:1 slope, before becoming insignificant at about $10H$ downstream. A_z profiles at sites in this wake region and which can be seen in Figure 3, tended to change their shape from that near the crest to one with a maximum value somewhat above ground level. The peaks in the A_z profiles can be seen to rise from ground level at the crest to approximately $Z/H = 1$ at between 5 to $10H$ downstream. The peak values of A_z at sites well downstream tended to be greater for the more gradual slopes where the wake was not so strong and the possibility of separation less likely. A sample comparison of these model data with the preliminary field tests by Bowen and Lindley (1974) is shown in Figure 5, together with the results from the theoretical solution described by Lindley *et al.* (1977). Although good agreement has been reached between the model and theoretical results, discrepancies in amplification factors are evident with the field results, particularly close to the ground. These differences highlight the problems of field testing where thermal effects and small irregularities in the terrain have a large effect on the local flow field.

5.2. TURBULENCE STRUCTURE

The RMS velocity variation, shown in Figure 6 as σ_u/\bar{V}_∞ , indicates that the wake generated behind the crest was also a region of high turbulence which dissipated as the flow proceeded downstream. Very little modification to the turbulence in the flow was evident outside this wake region. Jackson (1975) developed his theoretical model for the flow of a turbulent boundary layer over a low two-dimensional escarpment using a thin layer containing high Reynolds stresses, outside of which the flow was regarded as irrotational. This two-layer approach is similar in concept to the wake and undisturbed flow regions found in these model tests.

The variation in turbulence intensity σ_u/\bar{V}_z in Figure 7, was accentuated by the higher RMS velocities occurring in the regions of lower mean velocity. The turbulence intensity and the extent of the wake region increased with the slope angle of the

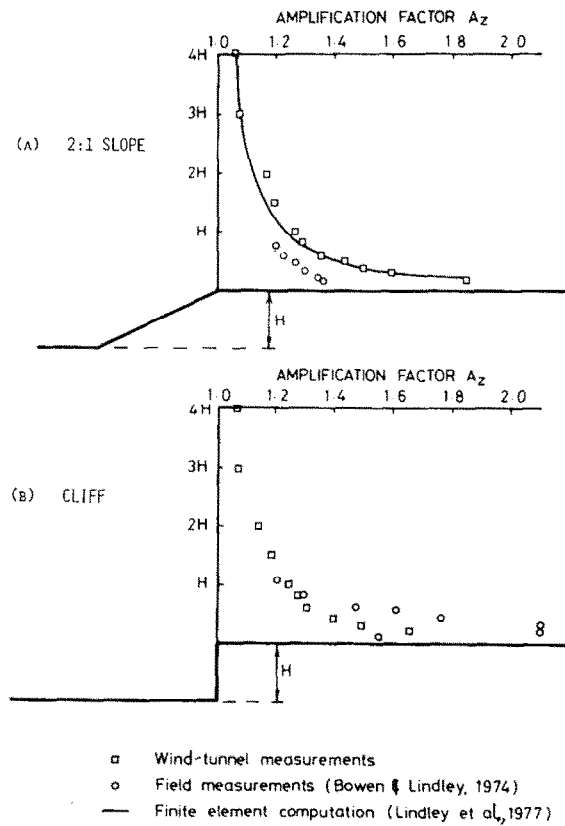


Fig. 5. A comparison of amplification factors obtained from the wind-tunnel tests with field data and with a theoretical solution.

escarpment. Outside the wake region, the small increase in flow speeds caused the intensity to be slightly reduced. Close upstream of the cliff and immediately downwind of the model crests close to the ground, there were regions where separated flows are normally expected. High turbulence intensities occurred in these regions and hot-wire measurements there could only be relied on to indicate trends due to their limitations in such flow conditions. The flows in these regions were not investigated and may be the subject of a separate study.

The non-dimensional turbulent energy spectra for several sites at $Z/H = 0.2$ are shown in Figure 8. A shift to higher frequencies is evident as the flow passed into the highly sheared region close behind the crest where small-scale turbulence was generated. This modification was lost as the flow continued farther downstream through the wake region. A similar comparison in Figure 9 for sites at $Z/H = 0.5$, which was practically outside the wake region, showed very little modification. The variation in the integral length scale of turbulence xL_u , at the same height ($Z/H = 0.2$) confirmed this trend to higher frequencies in the wake region. A value of $^xL_u = 85$ mm was measured at $1 H$ downstream of the cliff, compared with 140 mm

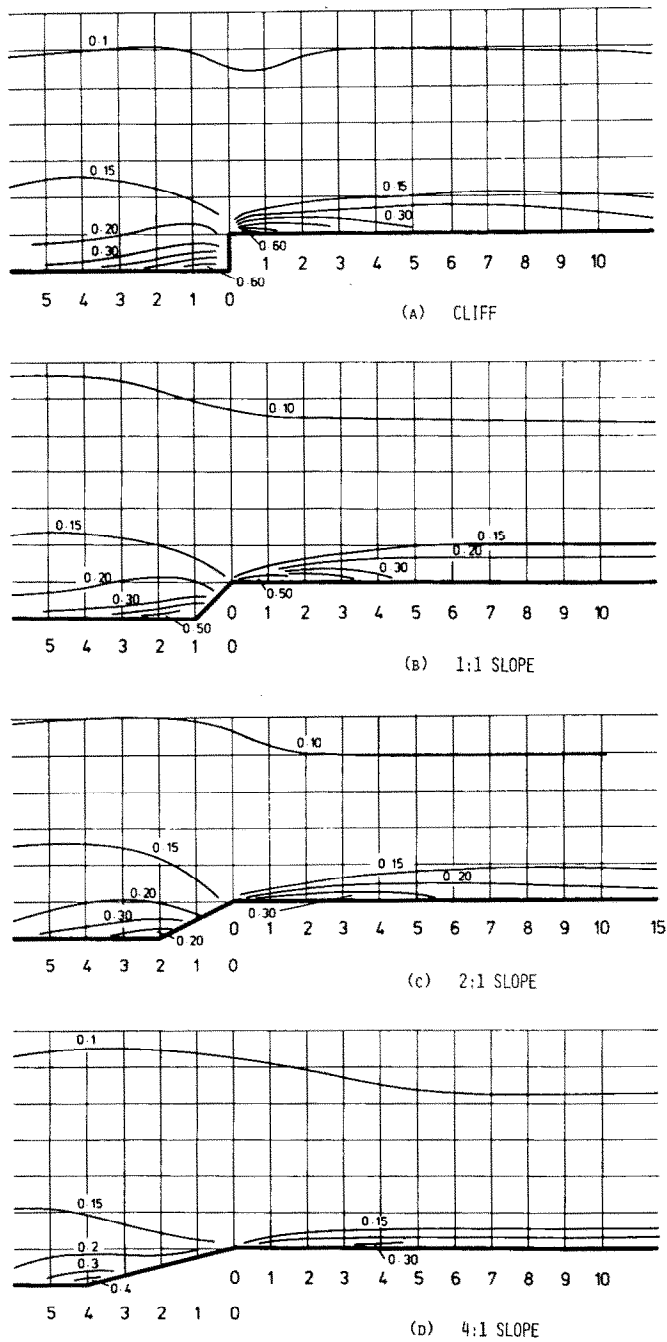


Fig. 7. (A)-(D) Contours of equal turbulence intensity σ_u / \bar{V}_z , over various escarpment slopes.

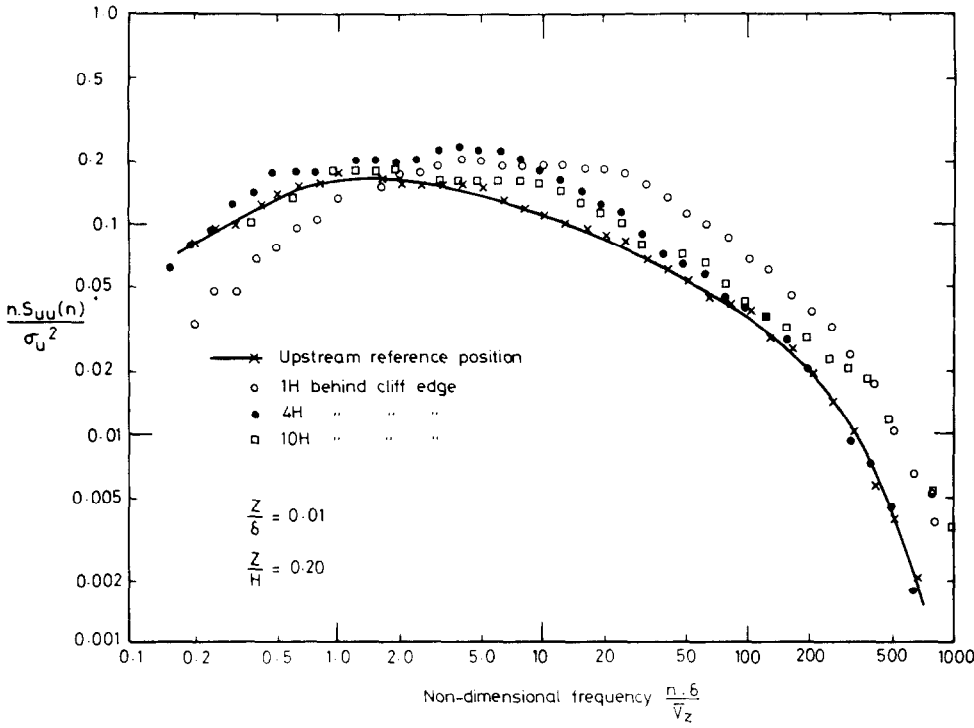


Fig. 8. Turbulent energy spectral densities at $Z/H=0.2$ above various locations over the cliff escarpment.

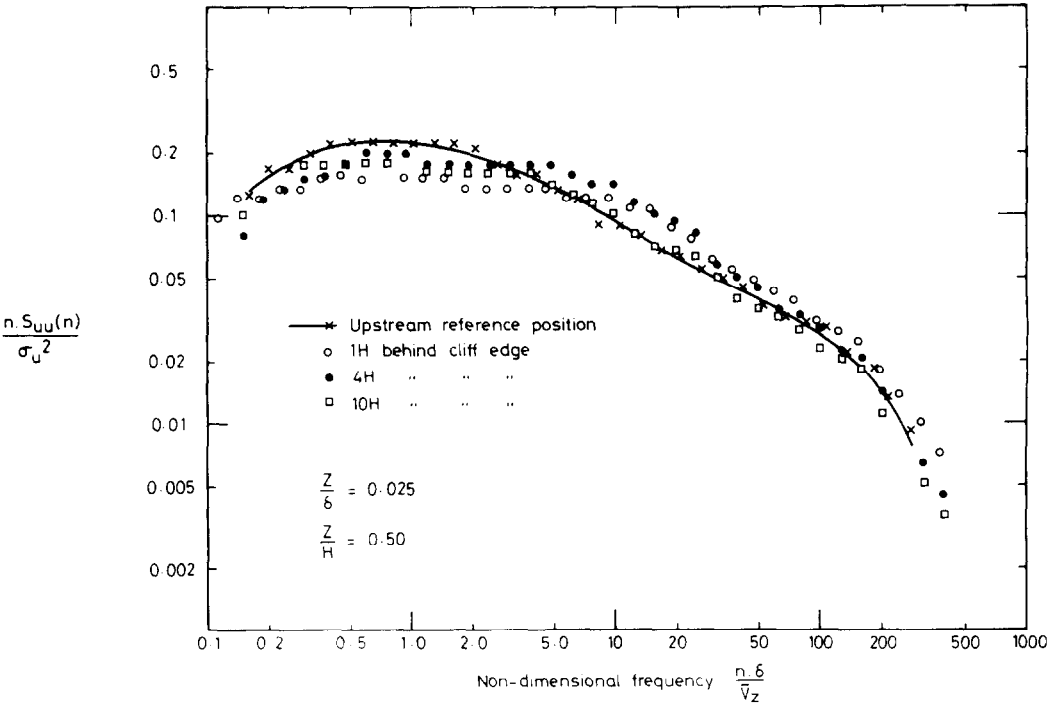


Fig. 9. Turbulent energy spectral densities at $Z/H=0.5$ above various locations over the cliff escarpment.

within the first three escarpment heights above the ground. The modification to the flow decreased rapidly with height from a maximum near the crest where $A_z \approx 1.8$, but persisted beyond ten heights downstream of the crest. A degree of shelter was noticed within five escarpment heights upstream of the slope. The variation in slope angle within the range considered had only a small effect on the mean flow behaviour.

A wake region characterised by higher turbulence intensities and lower mean flow speeds was noticed close to the ground, downstream of each crest. The turbulence intensity and the extent of the wake region increased with slope angle but weakened quickly in all cases to merge with the main flow after about ten escarpment heights downstream. A shift of the peak frequency in the turbulent energy spectrum towards higher frequencies, corresponding to a decrease in the turbulent length scale xL_u , was noticed for the flow entering the wake region close behind the crest, but this modification was lost as the wake developed. Outside the wake region, there was little change in the flow turbulence.

References

- Bowen, A. J. and Lindley, D.: 1974, 'Measurements of the Mean Wind Flow Over Various Escarpment Shapes', *Proc. Fifth Australasian Conference on Hydraulics and Fluid Mechanics*, University of Canterbury, N.Z., Dec. 1974, pp. 211–219.
- British Standard CP3: 1972, Chapter V, Code of Basic Data for the Design of Buildings, Part 2, Windloads.
- de Bray, B. G.: 1973, 'Atmospheric Shear Flows Over Ramps and Escarpments', *Industrial Aerodynamics Abstracts* 5, Sept.–Oct. 1973.
- ESDU 72026: 1972, 'Characteristics of Wind Speed in the Lower Layers of the Atmosphere near the Ground; Strong Winds (Neutral Atmosphere)', Engineering Sciences Data Unit, London.
- ESDU 74031: 1974, 'Characteristics of Atmospheric Turbulence near the Ground', Engineering Sciences Data Unit, London.
- Freeston, D. H.: 1974, 'Atmospheric Shear Flows Over Ramps and Escarpments', Presented to the Fifth Australasian Conference on Hydraulics and Fluid Mechanics, University of Canterbury, N.Z., Dec. 1974. Available from Mechanical Engineering Dept., University of Auckland.
- Jackson, P. S.: 1975, 'A Theory for Flow Over Escarpments', *Proc. Fourth International Conference on Wind Effects on Buildings and Structures*, Heathrow, U.K., September 1975. Cambridge University Press.
- Lindley, D., Bowen, A. J., and Morfee, P.: 1974, 'A Propeller Anemometer For a Digital Wind Data Acquisition System', *Proc. Fifth Australasian Conference on Hydraulics and Fluid Mechanics*, University of Canterbury, N.Z., Dec. 1974, pp. 258–268.
- Lindley, D., Bowen, A. J., and Morfee, P.: 1974, 'A Propeller Anemometer For a Digital Wind Data Atmospheric Boundary Layer', The Seventh CIB Congress and General Assembly, Edinburgh, Sept. 1977.
- Mitsuta, Y.: 1971, 'Characteristics of Airflow over the Barriers in the Storm', *Proc. Third International Conference on Wind Effects on Buildings and Structures*, Tokyo, 1971, pp. 33–44.
- New Zealand Standard 4203: 1976, New Zealand Standard Code of Practice for General Structural Design and Design Loadings for Buildings.
- Raine, J. K.: 1974, 'Simulation of a Neutrally Stable Rural Atmospheric Boundary Layer in a Wind Tunnel', *Proc. Fifth Australasian Conference on Hydraulics and Fluid Mechanics*, University of Canterbury, N.Z., Dec. 1974, pp. 190–199.
- Sacre, C.: 1973, 'Influence d'une Colline sur la Vitesse du Vent dans la Couche Limite de Surface', Internal Report, Centre Scientifique et Technique du Batiment, Nantes, France.
- WMO: 1964, *Sites for Wind Power Installations*, Technical Note No. 63, World Meteorological Organisation, Geneva.